

Disponible en [www.hormigonyacero.com](http://www.hormigonyacero.com)  
Hormigón y Acero, 2026  
<https://doi.org/10.33586/hya.2026.4149>

## ARTÍCULO EN AVANCE ON LINE

### ***Effect of Crumb Rubber on Fresh and Hardened Properties of Self-Compacting Concrete with Predictive Modeling***

Meyyappan PL, Anjali A

DOI: <https://doi.org/10.33586/hya.2026.4149>

Para ser publicado en: *Hormigón y Acero*

Por favor, el presente artículo debe ser citado así:

Meyyappan, P.L., & Anjali, A. (2026) Effect of Crumb Rubber on Fresh and Hardened Properties of Self-Compacting Concrete with Predictive Modeling, *Hormigón y acero*, <https://doi.org/10.33586/hya.2026.4149>

Este es un archivo PDF de un artículo que ha sido objeto de mejoras propuestas por dos revisores después de la aceptación, como la adición de esta página de portada y metadatos, y el formato para su legibilidad, pero todavía no es la versión definitiva del artículo. Esta versión será sometida a un trabajo editorial adicional, y una revisión más antes de ser publicado en su formato final, pero presentamos esta versión para adelantar su disponibilidad.

En el proceso editorial y de producción posterior pueden producirse pequeñas modificaciones en su contenido.

© 2026 Publicado por CINTER Divulgación Técnica para la Asociación Española de Ingeniería Estructural, ACHE

# Effect of Crumb Rubber on Fresh and Hardened Properties of Self-Compacting Concrete with Predictive Modeling

Meyyappan PL<sup>1</sup>, Anjali A<sup>1\*</sup>

<sup>1</sup>Centre for Building Materials, Department of Civil Engineering,  
Kalasalingam Academy of Research and Education, Krishnankoil – 626126

\*anjalia21546@gmail.com

**Abstract:** This research investigates the effect of crumb rubber on self-compacting concrete. Crumb rubber was incorporated as a substitute for coarse aggregate at 0–40% by volume. The study evaluated its impact on slump flow, passing ability, segregation resistance, compressive strength, split tensile strength, and flexural strength through laboratory testing. The results show that all mixes met the EFNARC slump flow criteria, with a marginal increase in deformability at higher crumb rubber contents. However, both the passing ability and stability decreased progressively beyond 20% replacement. Predictive models were developed using Genetic programming tool with high prediction accuracy ( $R^2 > 0.985$ ; RMSE = 0.09-1.10). The mechanical properties showed a systematic reduction, with the 28-day compressive strength retention reduced to 27.9% at 40% crumb rubber. Quadratic regression models were established to represent the strength degradation curves, that exhibited a high level of statistical correlation throughout the range of tested materials. The results indicate that there is a trade-off between improved behavior in the fresh (unhardened) state and reduced structural capacity. Moderate crumb rubber loading levels (10–20%) provide an optimal balance between workability, sustainability benefits, and mechanical properties while still requiring additional durability and microstructural validation for structural (load-bearing) applications.

**Keywords:** Self-Compacting Concrete, Crumb Rubber, Split Tensile Strength, Flexural Strength, Passing Ability, Regression Modeling, Genetic Programming tool.

## 1. INTRODUCTION

The growing pace of infrastructure development has further raised concerns about environmental sustainability, especially in the construction industry. Concrete production is known to be energy-intensive, with high CO<sub>2</sub> emissions from cement production and the use of natural aggregates. Current studies thus focus on the application of circular economy concepts and waste valorization to reduce the negative impacts on the environment [1,2,3]. Among the different types of solid waste, used automobile tires are a serious concern for the environment because of their non-biodegradable composition and the possibility of the release of toxic materials during improper disposal practices [4]. The recycling of waste rubber into construction materials has been identified as a potential approach for sustainable waste management [5].

Crumb rubber (CR), which is obtained from shredded used tires, has been extensively studied as a partial substitute for natural aggregates in concrete. [6] Various studies have shown that, although rubber addition could improve the ductility, impact resistance, and energy absorption capacity of concrete, the compressive, tensile, and flexural strengths are generally reduced due to the poor interfacial transition zones (ITZ) and the low stiffness of rubber particles [7,8,9]. Recent studies on rubberized concrete and rubberized self-compacting concrete (SCC) have also shown that the strength is reduced in proportion to the rubber content, although functional performance is improved in certain areas like non-structural components and vibration-sensitive structures [10,11,12].

SCC is a highly flowable concrete that can consolidate under its own weight without the need for mechanical vibration, providing better filling ability and passing capacity in congested

areas of reinforcement [13,14]. Although SCC improves construction efficiency and quality control, it is not necessarily economical because of the increased cost of admixtures; [15] instead, its benefits are in performance and improved properties [16]. The addition of CR to SCC introduces more rheological challenges, as SCC must have a balanced combination of viscosity, segregation resistance, and flowability. Research works involving the combination of CR with supplementary materials like fly ash, nano-silica, and calcium-based materials have demonstrated that combined modifications can counteract strength reduction, but the balance between fresh and mechanical properties is still difficult to achieve [17,18].

Although a vast amount of research has been conducted on rubberized SCC, there is still a need for the systematic investigation of high-volume coarse aggregate replacement (up to 40%) under European Federation of National Associations representing producers and applicators of specialist building products (EFNARC) based rheological control, and at the same time, developing effective predictive models for mechanical properties [19]. The existing models, such as response surface methodology, have been mainly used for optimization purposes within a restricted parametric domain [20,21], and there is still room for symbolic modeling approaches that can interpret non-linear strength degradation behavior.

The driving force behind this study stems from the recognition of the simultaneous need to (i) enhance environmental sustainability by efficiently reutilizing waste tires and (ii) design a technically valid rubberized SCC mix that preserves acceptable workability while also attempting to quantify the unavoidable strength-related property loss. In view of the fact that the addition of CR is known to reduce the compressive, split tensile, and flexural strengths, this research study does not aim to represent CR as a strength-gaining material. Therefore, this research aims to explore the impact of 10-40% replacement of coarse aggregates with CR on the fresh and hardened properties of SCC. Moreover, a Genetic Programming (GP) model is proposed to predict the compressive strength at 7 days and 28 days, split tensile strength, and flexural strength in terms of the amount of CR. The proposed model is designed to focus on predictive accuracy rather than curve fitting, achieving high accuracy ( $R^2 > 0.985$ ) for the nonlinear relationships. This research integrates experimental analysis with symbolic modeling to make a significant contribution to the field of rubberized SCC.

This study offers three major contributions to the literature of sustainable concrete technology. Initially, it presents a comprehensive experimental study on the use of CR as a coarse aggregate substitute (10-40%) in SCC to accurately quantify its effects on rheological properties and strength degradation, in strict compliance with EFNARC specifications. Secondly, it reveals an optimal replacement range of (10-20%) that strikes a balance between environmental sustainability and structural performance, without exaggerating the latter. Thirdly, it proposes a highly accurate GP-based predictive model that accurately represents the nonlinear relationship between CR content and mechanical properties.

## **2. MATERIALS AND METHODS**

This section will discuss about the materials that were used, the mix designs methodology, an experimental program for assessing both the fresh and hardened behavior of the materials, and the predictive modeling framework created to statistically define the strength variability resulting from incorporating CR into SCC mixtures.

### **2.1 Materials**

The constituent materials utilized in this research such as cement, fine aggregate, coarse aggregate, CR as partial aggregate replacement and chemical admixtures as well as the physical properties of these constituents are described in the following section, along with applicable standards of selection and characterizing the aforementioned constituents.

### **2.1.1 Cement**

Grade 53 Ordinary Portland Cement (OPC) was the main binder used in all the mixtures, and it conforms to the specifications of IS 12269. The choice of OPC 53 was made based on its early strength development and its popularity in structural concrete work in India, which meets the requirements of performance-based SCC. The specific gravity of the cement was 2.90, and the standard consistency was 32%. The initial and final setting times were within the limits specified by IS norms. The high clinker content in OPC 53 ensures sufficient early strength development, which is essential in rubberized mixes, as strength is expected to decrease. The chemical composition of the cement, obtained from the manufacturer, mainly consisted of CaO, SiO<sub>2</sub>, Al<sub>2</sub>O<sub>3</sub>, and Fe<sub>2</sub>O<sub>3</sub>. All of the cement was stored dry to ensure that moisture did not cause differences between batches.

### **2.1.2 Fine Aggregate**

Natural river sand, a fine aggregate for the concrete was obtained from the Kollam region in India. The sand satisfied IS 383 standards and fell under the permissible limits of grading for concrete production. The specific gravity of the sand was 2.65, and the bulk density was about 1745 kg/m<sup>3</sup>. The water absorption was 1.2%, and the fineness modulus was 2.68, which was suitable for SCC use. Sieve analysis was carried out as per IS 2386 (Part I), and the graph showing the particle size distribution is given to show compliance with grading standards. The correct grading of fine aggregates is vital for SCC because it provides sufficient filling characteristics and minimizes the risk of segregation during mixing.

### **2.1.3 Coarse Aggregate**

The coarse aggregate used in this study consisted of crushed granite aggregates with a nominal maximum size of 12.5 mm. The coarse aggregate met the IS 383 requirements for graded coarse aggregates in structural concrete. It had a specific gravity of 2.83, a bulk density of approximately 1600 kg/m<sup>3</sup>, and a water absorption of 0.6%. The fineness modulus of this aggregate was found to be 7.16. Gradation analysis was performed using the procedure defined by IS 2386 (part I), and a particle sizing graph is presented to demonstrate that the crushed aggregates meet the standard limits for grading. The crushed aggregates also enhance mechanical interlocking between the cement matrix and the aggregates due to their angular shape and rough surface texture, resulting in improved bond strength. In addition, all aggregates were dried in ovens prior to mixing to reduce variability caused by water in the binder-water ratio due to variations from moisture present in the aggregates during mixing.

### **2.1.4 Crumb Rubber**

CR generated from shredding old vehicle tires, is a cheap substitute for coarse aggregate in concrete. Figure 1 shows the CR where the average size of the rubber be 10–12.5 mm similar to the nominal size of the coarse aggregate that it is replacing. The approximate density of CR is about 1100 kg/m<sup>3</sup> (about 70% less than natural aggregate), which has to be considered in whatever replacement method is chosen. The absorption of water by CR is less than 1% and the modulus of elasticity of the rubber is also relatively low compared to mineral aggregates. The rubber is an irregular shape and the surface is generally smooth, which could reduce the strength of the ITZ between the two materials. There was no chemical pre-treatment for CR as it was used in a dry state. The replaceable aggregates were replaced based on the mass of coarse aggregate with a direct reduction of natural aggregate.



**Figure 1:** CR derived from waste tires, used as a sustainable partial replacement for natural coarse aggregate in SCC mixes

### **2.1.5 Chemical Admixtures**

CERA Hyperplast XR-W40, a high-range water reducing (superplasticizer) conforming to ASTM C494 Type F, was used as an admixture to achieve SCC with the required flowability without increasing water content [23]. This superplasticizer (SP) had a specific gravity of 1.06 - 1.12 and was chloride free making it suitable for use in any application involving reinforced concrete. The dosage for this high-range water-reducing (SP) used during trial optimization ranged from 0.3% to 1.5% by weight of cement. Viscosity modifying agent (Master Matrix VMA 362) was also added as a modifier to enhance the segregation resistance and maintain the cohesiveness of highly flowing mixes. This viscosity modifying agent (Master Matrix VMA 362) had a density of approximately 1.002 g/cm<sup>3</sup>, and dosages ranged from 0.3% to 0.8% by weight of cement. Both of these admixtures were compatible with OPC, creating a stable rheological performance through the use of rubberized SCC systems.

## **2.2 Mix Design Methodology**

The following section describes the proportioning approach used in the design of SCC mixtures with different levels of CR replacement, including criteria for the selection of materials, volumetric adjustments, EFNARC compliance, and approaches used for the evaluation of fresh and hardened concrete properties.

### **2.2.1 SCC Reference Mix**

The reference SCC mix was created according to the EFNARC (2005) method of defining a mixture that met the criteria for fill-ability, passing ability, and resistance to separation [22]. A series of five trial mixes (from SCC1 to SCC5) were developed by varying the amount of SP and viscosity-modifying agent (VMA) while keeping the amount of cement, fine aggregates, and coarse aggregates constant. The water-to-binder (W/B) ratios were adjusted at a controlled level to achieve target slump flow (650-800 mm), V-funnel time (6-12 s) and L-box ratios of 0.8 or greater. The final permissible SCC reference mix (SCC5) was selected because it produced the best fresh-state performance within the EFNARC limits. SCC-CR0, is the optimized mix which serves as a control mixture for subsequent CR replacement.

### **2.2.2 CR Replacement Strategy**

CR were used to partially replace coarse aggregate at 10%, 20%, 30%, and 40% based on the mass of the coarse aggregate. This rubber crumbs have lower density than natural aggregates

so the method of replacement would have meant an increase in aggregate volume and a decrease in mixture density. Coarse aggregate content would, therefore decrease at an equal rate as courses are increased in percentage by using rubber crumbs.

In order to isolate the effect of using rubber crumbs on fresh and hardened properties, the admixture dosages and water contents from the evaluated SCC-5 mix were all kept the same; thus, providing no direct means of inferring the effect that rubber crumbs had on the W/B ratio from any of the test variables. Table 1 shows the different mixing proportions of SCC by replacing CR.

**Table 1:** Mix Proportions of SCC with CR Replacement

Mix ID	Cement (kg/m <sup>3</sup> )	FA* (kg/m <sup>3</sup> )	Natural CA (kg/m <sup>3</sup> )	CR (kg/m <sup>3</sup> )	Water (kg/m <sup>3</sup> )	SP (kg/m <sup>3</sup> )	VMA (kg/m <sup>3</sup> )	W/B Ratio
SCC-CR0	6.42	9.24	15.00	0.00	3.80	0.10	0.05	0.59
SCC-CR10	6.42	9.24	13.50	1.50	3.80	0.10	0.05	0.59
SCC-CR20	6.42	9.24	12.00	3.00	3.80	0.10	0.05	0.59
SCC-CR30	6.42	9.24	10.50	4.50	3.80	0.10	0.05	0.59
SCC-CR40	6.42	9.24	9.00	6.00	3.80	0.10	0.05	0.59

(\*FA-Fine Aggregate)

All the constituents of the mix were standardized in terms of kg/m<sup>3</sup>. The water content was standardized from liters to equivalent units based on the assumption of unit density. In addition, the superplasticizer and VMA content were standardized from percentage to equivalent units based on the content of the cement. As rubber crumb content increases, there is a decrease in the total weight of aggregate due to its lower density. This strategy ensures that, the effect of rubber crumb content can then be evaluated without confounding admixture variations.

## 2.3 Experimental Program

This section describes the specimen preparation, curing conditions, and standardized tests conducted to determine the fresh properties (slump flow, L-box, stability) and hardened mechanical strengths (compressive strength, split tensile strength, and flexural strength) at 7 and 28 days for different levels of replacement of CR.

### 2.3.1 Mixing Procedure

All concrete mixes were mixed in a laboratory pan mixer with a 50 L capacity to ensure uniform blending, and all mixing procedures were standardized, which allowed for less variability. In each batch the cement, fine aggregate, and natural coarse aggregate materials were dry-mixed together for 2 minutes to obtain a homogeneous mixture prior to adding CR (wherever it is applicable) and mixing an additional 1 minute to ensure that the CR was uniformly distributed. Then, approximately 70 % of the water pre-mixed with SP was gradually added, and mixed it for 2 minutes. The remaining water containing the VMA was then added and mixed together for 2 to 3 minutes. Each batch was mixed for approximately 7 to 8 minutes. The fresh concrete was maintained at a temperature of  $27 \pm 2$  degrees Celsius, and no external vibration was used when casting, which is consistent with SCC principles.

### 2.3.2 Fresh Property Tests

According to EFNARC 2005 guidelines (European Federation of National Associations of Manufacturers of Product for the Construction Industry), fresh state properties of SCC were researched using slump flow diameter and T50 time measurements to determine filling properties and flow consistency. The acceptable slump flow range for the study is 650 - 800 mm. V-Funnel testing was used to evaluate both flow time and viscosity characteristics, with acceptable V-Funnel test times ranging from 6 - 12 seconds. To evaluate passing ability, the L-box was used to record the ratio of height ( $H_2$ ) to height ( $H_1$ ); a minimum value of 0.80 for  $H_2/H_1$  indicates that adequate passing will occur within congestion because of reinforcement. All tests were completed immediately after the completion of mixing. Each measurement was made in triplicate as to validate the results. A summary of the standards and acceptance criteria for testing SCC are presented in Table 2.

**Table 2:** Fresh Property Tests and Standards

Test	Standard/Guideline	Acceptance Criteria
Slump Flow	EFNARC (2005)	650–800 mm
V-Funnel	EFNARC (2005)	6–12 s
L-Box	EFNARC (2005)	$\geq 0.80$

### 2.3.3 Specimen Preparation and Curing

Without any mechanical vibration, the Concrete specimens were allowed for self-compaction under gravity. The cube molds which are 150 mm x 150 mm x 150 mm and according to IS 516 were used to test compressive strength of concrete. Split tensile strength was tested using cylinder specimens which were 150 mm diameter and 300 mm height according to IS 5816. Flexural strength was tested using prisms which had dimensions of 100 mm x 100 mm x 500 mm according to IS 516. After  $24 \pm 2$  hours specimens were removed from the molds and were cured in a water tank maintained at  $27 \pm 2$  °C until the designated testing ages of 7 to 28 days. For each mix a minimum of 3 specimens were tested for each mechanical property to provide statistical reliability in reporting average values. Figure 2 shows the overall methodology employed in mixing, casting, and fresh-state testing of SCC mixtures.



**Figure 2:** Experimental procedure: mixing, casting, and fresh-state testing (slump flow and L-box) of SCC mixtures

### 2.3.4 Hardened Property Tests

A calibrated compressive strength testing machine (CTM) with a capacity of 2000kN, in accordance with IS 516, was used to assess compressive strength by using a continuous load at a uniform rate of 0.6 MPa per second until failure (Figure 3). The split tensile strength test was performed according to the principles set out in the IS 5816 standard. This test was conducted with the application of steady state diametral load. The flexural strength test (i.e., modulus of rupture) was carried out in accordance with third point loading as per IS 516 standards with controlled continuous loading to provide a uniform stress distribution of load. All tests were performed at 7 days (approximately early age) and at 28 days (standard design age) to evaluate the strength of the concrete. All failure modes were inspected visually for assessing the failure of the test specimens, including an assessment of cracking patterns and bonding behavior, particularly at the higher levels of CR replacement.

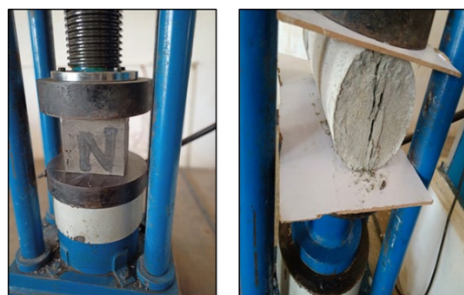


**Figure 3:** Experimental setup for hardened-state testing: compressive, split tensile, and flexural strength evaluation of SCC specimens

## 2.4 Predictive Modeling Framework

This section describes the construction of a GP-based predictive model to quantify the nonlinear relationship between the percentage of CR replacement and SCC mechanical properties.

### 2.4.1 Modeling Approach and Rationale

A data-driven predictive framework based on GP was created to model the nonlinear relationship between CR replacement percentage and the mechanical properties of SCC in conjunction with an experimental research study. GP models nonlinear relationships between the two variables; however, unlike traditional regression methods that assume a functional form, GP is an evolutionary symbolic regression method that evolves the best-fit mathematical expression for the data points. GP is well suited for modeling rubberized concrete because of the nonlinear degradation of the rubberized concrete strength due to the disparity in density, degradation of the ITZ, and increased porosity of the concrete.

The use of GP in this study was not only to fit a trend but to produce intelligible predictive equations that provide the ability to estimate the compressive strength, split tensile strength, and flexural strength of SCC for 7 and 28 days based on the CR replacement percentage. One independent variable, CR replacement percentage (0-40%), and six dependent bubbles will calculate the strength of SCC based on compressive strength, split tensile strength, and flexural strength at two different curing times. The dependent output variables were defined as 7-day compressive strength ( $f_{cs7}$ ), 28-day compressive strength ( $f_{cs28}$ ), 7-day split tensile strength ( $f_{ts7}$ ), 28-day split tensile strength ( $f_{ts28}$ ), 7-day flexural strength (ffs7), and 28-day flexural strength (ffs28) and the expression for those variables are,

$$f_{cs7} = 39.5 - 0.82x + 0.003x^2 \quad (1)$$

$$f_{cs28} = 49.2 - 0.89x + 0.004x^2 \quad (2)$$

$$f_{ts7} = 6.35 - 0.055x + 0.0004x^2 \quad (3)$$

$$f_{ts28} = 7.48 - 0.065x + 0.0005x^2 \quad (4)$$

$$f_{fs7} = 6.48 - 0.058x + 0.00045x^2 \quad (5)$$

$$f_{fs28} = 7.18 - 0.044x + 0.00038x^2 \quad (6)$$

The goal of the modeling process was to minimize prediction error while maximizing the simplicity of the equations to provide a practical solution for mix design optimization.

### 2.4.2 Model Development and Data Handling

Model development was based on an experimental dataset from five mixes, from CR0 through CR40. The dataset includes average values of compressive strength, split tensile strength, and flexural strength after 7 days and 28 days for each mix configuration. All inputs were normalized before training the model in order to eliminate scale dominance. GP was carried out using a symbolic regression function with the following control parameters: population size = 100, maximum generation = 500, crossover probability = 0.85, mutation probability = 0.10, and tournament selection method.

K-fold cross-validation,  $k = 5$  was used due to the limited dataset size to ensure that the model is predictive. To measure prediction quality, three different metrics were used based on model performance, they are coefficient of determination ( $R^2$ ), root mean square error (RMSE), and mean absolute percentage error (MAPE). A summary of the modeling inputs, evaluation metrics, and resulting outputs are included in Table 3 below.

**Table 3:** Modeling Inputs and Performance Metrics

Category	Description
Input Variable	CR replacement (%)

Output Variables	$f_{cs7}, f_{cs28}, f_{ts7}, f_{ts28}, f_{fs7}, f_{fs28}$
Evaluation Metrics	$R^2, RMSE, MAPE$
Validation Method	5-fold cross-validation

The framework is aimed at providing confidence in the transparency and repeatability of the statistical reliability associated with the predictive outputs.

### **2.4.3 Model Validation and Predictive Performance**

The GP models were able to capture a high level of consistency between predicted and experimental values for all strength parameters. The values of the coefficient of determination were above 0.985 for all six models, which is an excellent level of goodness of fit. The RMSE values varied between 0.09 and 1.10 MPa, which further supports the low prediction error in relation to experimental variability. Notably, the symbolic expressions derived using GP captured the quadratic relationship between strength degradation and the increase in CR content, which is a manifestation of the nonlinear mechanical response of rubberized SCC.

The residual plots indicated the absence of systematic errors at all levels of replacement, which is an important aspect in confirming that the models have predictive capabilities and do not suffer from overfitting. The curvature terms in the symbolic expressions derived using GP describe the net effects of decreased stiffness, ITZ degradation, and volumetric changes associated with the addition of CR. The GP-based framework provides an interpretable and useful decision-support tool for strength performance estimation at different levels of CR dosages without requiring extensive experimental work.

## **3. RESULTS AND DISCUSSION**

This subsection presents the findings of our statistical evaluation about the fresh and hardened properties of CR modified SCC and examines performance trends and trade-offs. It will also evaluate the effectiveness of the predictive modeling results based on the differences between experimental (actual) and predicted (simulated), as well as the use of regression-based methods for validating these predictions.

### **3.1 Statistical Framework and Data Reliability**

To maintain the analytical rigor and reproducibility, all experimental results have been presented as the mean  $\pm$  standard deviation (SD) based on  $n = 3$  test mixes per test (test spec), consistent with the protocol for testing of standard concrete materials. The averaging of experimental results allows for the quantitative evaluation of the dispersion (variability), as well as the minimization of possible bias in interpreting marginal differences of performance among the CR replacement levels. The coefficient of variation (COV) was kept at an acceptable experimental limit ( $<10\%$  for strength tests) for all tests, which indicates that the tests were repeatable and that the test specimens are built uniformly.

Error bars ( $\pm 1$  SD) were used in the graphical depiction of the average performance data to provide a visual basis for the statistical comparison. The average performance data for each test period was adjusted for percentage variation (%) from the control mix (CR0), to normalize the test performance trends of the mixes.

All predictions based on the analysis of the experimental performance data are shown as descriptive curve fits of five experimental data points and should not be used to predict beyond the limits established by the experimental test program.

## 3.2 Fresh-State Properties

### 3.2.1 Slump Flow and Flowability

The slump flow of SCC with 0% to 40% CR was measured three times independently ( $n=3$ ) to obtain the values as shown in the Figure 4 as mean  $\pm$  SD for each set of mixtures. All mixtures met the EFNARC criteria for rheological properties, which require a slump flow range of 650 to 800 mm, indicating they would fill the form without difficulty. The control mixture (SCC-CR0) has a slump flow of  $690 \pm 5$  mm, while the addition of 10% CR increased the slump flow to  $700 \pm 6$  mm (+1.45%). The slump flow for SCC-CR20 was equal to that of the control mix ( $690 \pm 4$  mm), and the slump flow at SCC-CR30 was very slightly increased ( $695 \pm 5$  mm; +0.72%). The slump flow was highest for SCC-CR40 ( $710 \pm 7$  mm; +2.90%) due to increased fluidity at the higher CR levels. Although SCC with more CR provided a greater mean value of slump flow, the overlap in the SDs suggest there are no statistically significant differences between the slump flows of the mixtures with 0% to 30%. The increased mean slump flow of SCC-CR40 was due to a decreased aggregate interlock (cohesion) and decreased particle stiffness at this CR level and not due to an increase in rheological stability. Slump flow is only an indicator of deformability (flowability) of SCC. Therefore, it should not be interpreted as an indicator for the passing ability or segregation resistance of SCC.

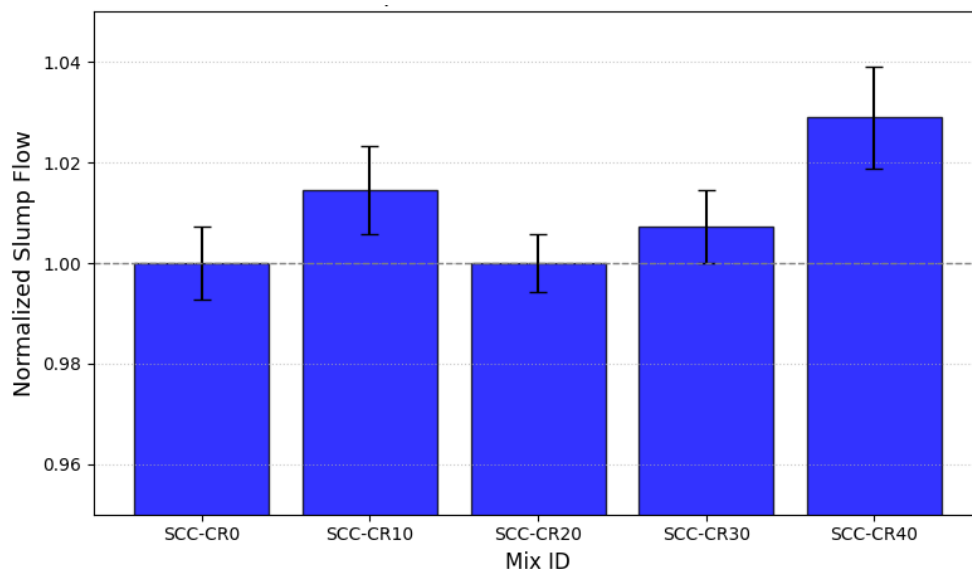


**Figure 4:** Normalized slump flow of SCC with varying crumb rubber content. Values represent mean  $\pm$  SD ( $n = 3$ ), normalized with respect to the control mix (SCC-CR0).

### 3.2.2 Passing Ability (L-Box Test)

The L-Box test was evaluated to assess the passing ability of SCC mixed with CR. For each concrete mix, a ratio of  $H_2/H_1$  has been calculated and reported as mean  $\pm$  SD ( $n=3$ ). As per EFNARC guidelines, the ratio must satisfy  $H_2/H_1 \leq 1.0$ . The test results show that SCC-CR10 to SCC-CR30 meet the EFNARC minimum requirement ( $\geq 0.80$ ), indicating satisfactory passing ability. However, SCC-CR40 had a ratio of  $0.70 \pm 0.04$ , violating the limit, which indicates possible blocking in congested reinforcement. It is important to note that passing ability and slump flow are two different parameters. Although SCC-CR40 showed higher slump flow, its L-box ratio clearly indicates poor passing ability. Error bar chart as shown in Figure 5 were used to denote variability in L-Box test passes and to avoid any further interpretation of the marginal differences.

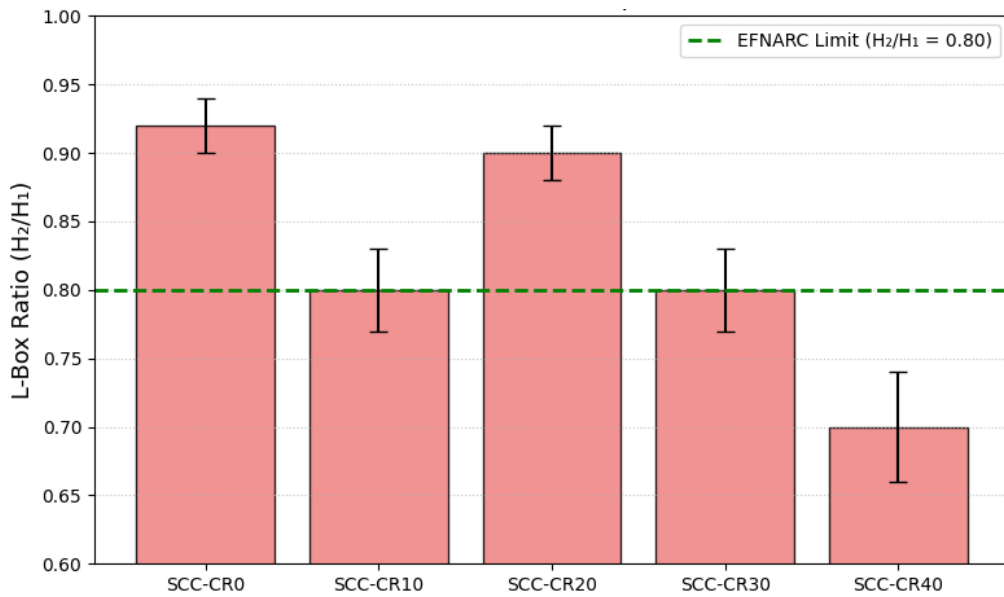


**Figure 5:** L-box ratio of SCC mixtures with varying crumb rubber content. Values represent mean  $\pm$  SD ( $n = 3$ ). The dashed line indicates the EFNARC recommended limit.

### 3.2.3 Stability and Segregation Resistance

Visual stability assessment was used to determine the segregation resistance of SCC mixes, following the EFNARC guidelines. No segregation tests were conducted on sieves prior to slump flow and L-Box testing, so visual inspection was used to assess stability at the time of testing. A qualitative rating scale was used to note observations (0 = no visible segregation; 1 = minor mortar halo; 2 = significant aggregate settlement). Figure 6 shows the obtained results. A decrease in stability was observed with an increase in carbon ratio (CR) content. Both SCC-CR0 and SCC-CR10 displayed very high levels of cohesion, with no visible segregation. Mortar separation was noted at 20% CR and 30%, with SCC-CR40 showing many signs of instability. Thus, the claim of "no segregation" holds true for mixes with visual evidence for that assertion. A quantitative segregation test should be performed in future investigations to reinforce this finding.

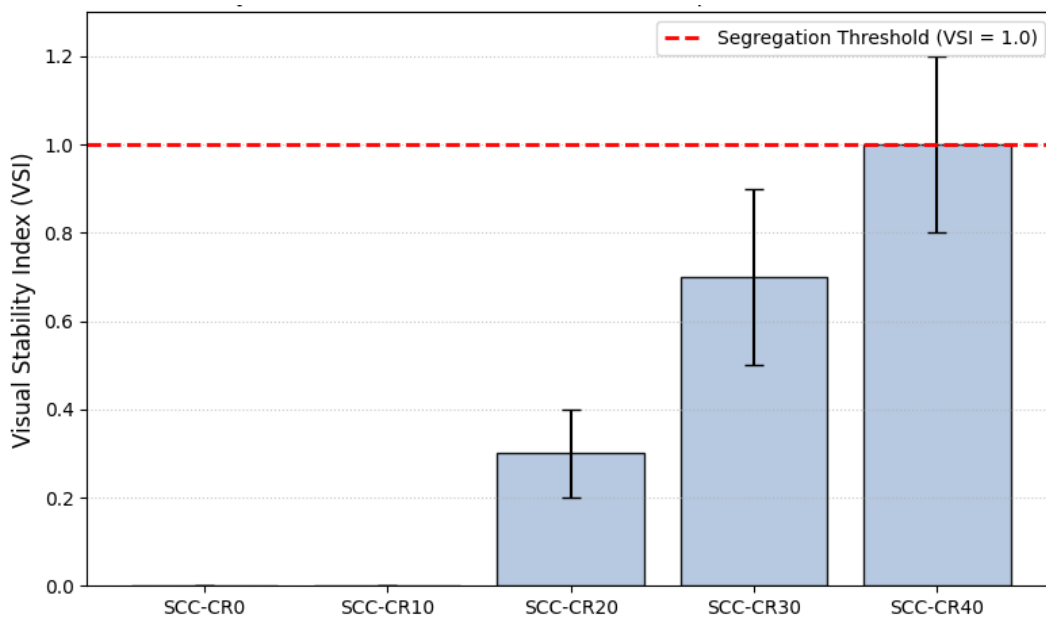


**Figure 6:** Visual stability index of SCC mixtures with varying crumb rubber content. Values represent mean  $\pm$  SD (n = 3).

### 3.3 Hardened Mechanical Properties

#### 3.3.1 Compressive Strength

The compressive strength was measured at 7 days and 28 days for each mix using three specimens (n = 3). Results shown in Figure 7 were reported as means  $\pm$  SD values, as well as to promote statistical transparency and prevent over-interpreting marginal differences. Across both curing ages, an increase of CR led to a reduction in compressive strength; this reduction in strength was statistically consistent, as evidenced by the low SDs observed. This reduction is due to the reduced rigidity of rubber particles and reduced aggregate-matrix interaction, and not due to any crack-bridging effect. All different types of mixes exhibited strength gains from 7 day to 28 day, however the presence of CR in each mix substantially restricts any load-bearing capacity and, thus, the only performance improvements that may be attributed to each mix were associated with workability and not compressive strength.

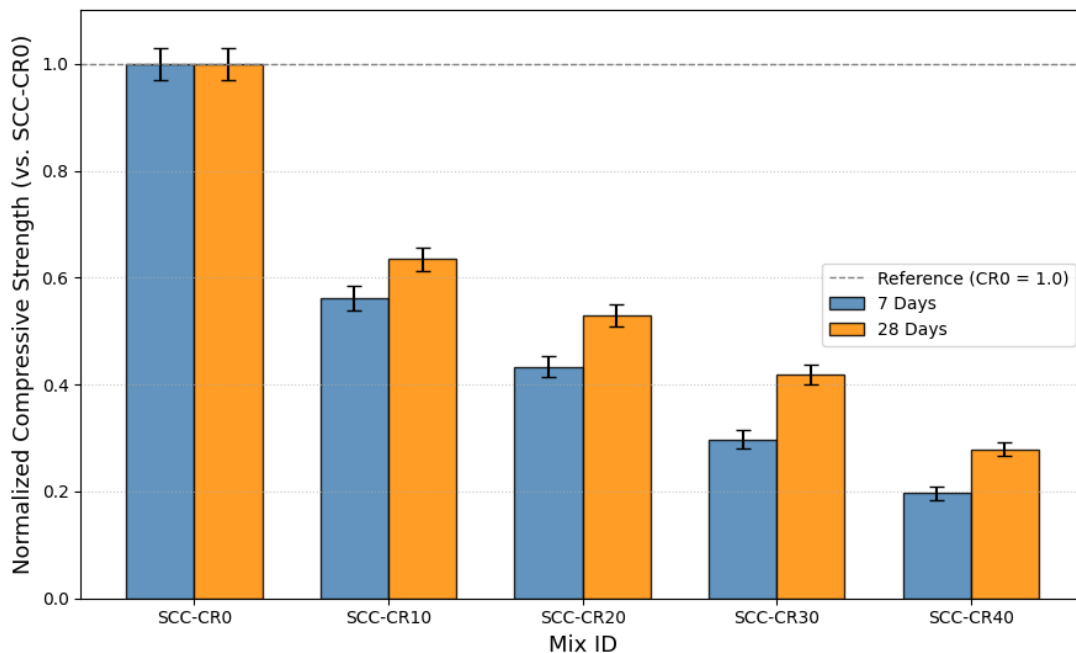


**Figure 7:** Normalized Compressive Strength of SCC with CR at 7 and 28 Days with  $\pm 1$  SD Error Bars

#### 3.3.2 Split Tensile Strength and Flexural Strength

Split tensile and flexural strengths were assessed at 7 and 28 days (n=3), and the results were reported as the average  $\pm$  SD in order to verify that they are statistically valid. Figure 8 shows the result where both the tensile and flexural strengths decreased with an increase in the CR content. And the Shaded regions showing  $\pm 1$  SD around each line. At 28 days, the split tensile strength decreased by about 36% when comparing the CR40 to CR0, while the flexural strength decreased by about 25%, indicating that there may be some improvement in deformability compared to an increase in load bearing ability. There is no evidence of a crack-bridging mechanism because no microstructural verification was performed. The predominant cause for the reduction in strength is attributable to the lower rigidity of the rubber aggregate and poor

interfacial adhesion between the rubber aggregate and the cement matrix. Variability remains within acceptable limits in accordance with the experiment (low SD), thereby supporting the consistency of the data with respect to the intended trends.

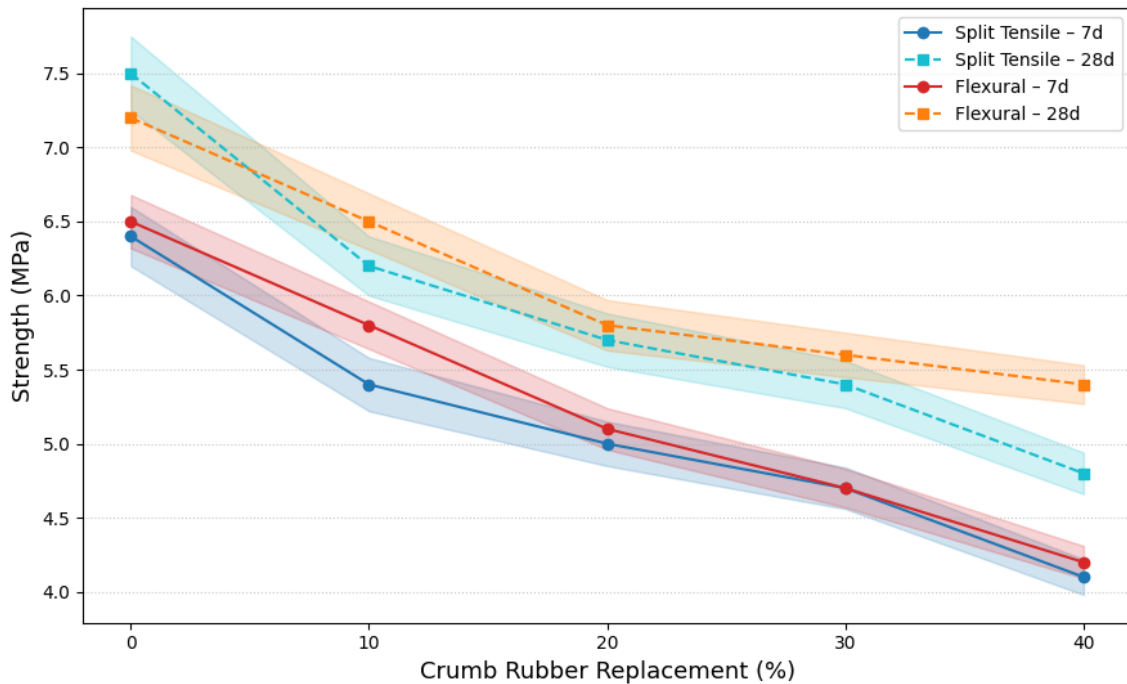


**Figure 8:** Split Tensile and Flexural Strength of SCC with CR Replacement with  $\pm 1$  SD Error Bands

### 3.4 Comparative Performance Analysis

To assess the overall effect of CR, the fresh and hardened properties were normalized against that of the control mix (SCC-CR0). Only 28-day mechanical strengths analysis was performed to evaluate potential structural properties as recommended by performance standards. Obtained results are illustrated in Figure 9. The slump flow retention rates were consistently at or slightly above the 100% mark indicating no loss of deformability of the mix. However, the compressive strength was significantly lower as compared to the control mix; at different levels of CR, specifically CR40. The compressive strength was 27.9% of the control mix. Tensile or flexural strengths were less affected when compared to the compressive strength. The passing ability decreased progressively with the highest level of CR40 falling below the EFNARC standards for acceptable passing ability. The results support that while workability of the mix is retained; the structural capacity of the mix is greatly reduced with increasing amounts of CR. Though CR10–CR20 exhibited moderate strength reduction while maintaining acceptable workability; however, further evaluation of durability and long-term performance is required before structural application.

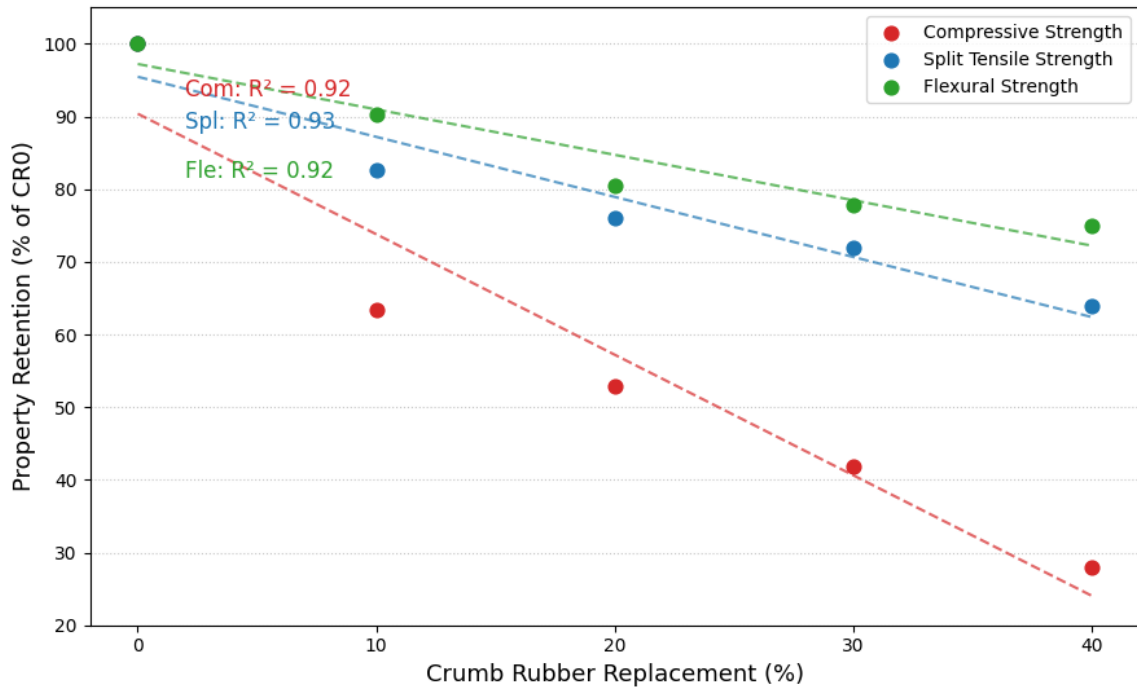


**Figure 9:** Normalized Performance Relative to SCC-CR0

### 3.5 Predictive Modeling Evaluation

#### 3.5.1 Model Development and Statistical Adequacy

To model the relationship between the replacement amount of CR with 28-day compressive strength (i.e., to develop a quadratic polynomial regression model), data from five trials (i.e., 0 – 40% CR) was used. Summary of the statistics are provided in Table 4. The high  $R^2$  value indicates a strong correlation exists between the amount of CR and the reduction in the strength of the specimen for the tested range. This correlation, however, may only be valid for the limited number of data points used, and represents a descriptive curve fit, as opposed to providing a mechanistic explanation for or a generalizable prediction of CR on compressive strength. Additionally, there are no physical interpretations provided for any of the regression coefficients. Therefore, this model accurately reflects the non-linear trend describing the degradation of compressive strength due to the addition of CR, but results must be interpreted with caution. However, this model should not be extrapolated beyond the tested range.

**Table 4:** Regression Model Statistics for 28-Day Compressive Strength

Parameter	Value
Model Type	Quadratic Polynomial
Number of Data Points	5
$R^2$ (Coefficient of Determination)	0.98
Adjusted $R^2$	0.97
RMSE (MPa)	1.12
Standard Error of Estimate (MPa)	1.05

#### 3.5.2 Compressive Strength Modeling (28 Days)

The quadratic regression model was created with the experimental data for five-point (0-40% CR) in order to establish the correlation between the amount of CR and the 28-day compressive

strength. The model had a high coefficient of determination ( $R^2 = 0.984$ ), as well as a small RMSE (1.12 MPa), demonstrating a high level of statistical agreement across the range tested. All absolute prediction errors less than 1 MPa and were similar in magnitude to the experimental SDs, providing confirmation of acceptable descriptive accuracy. The regression used is a curve-fit exercise rather than a mechanistic model. The regression is based on a relatively small number of data points; therefore, users should exercise caution while interpreting this model. This model cannot be used to predict past any point beyond the range it has been tested. Figure 10 illustrates a comparative analysis of both experimental and predicted compressive strength.

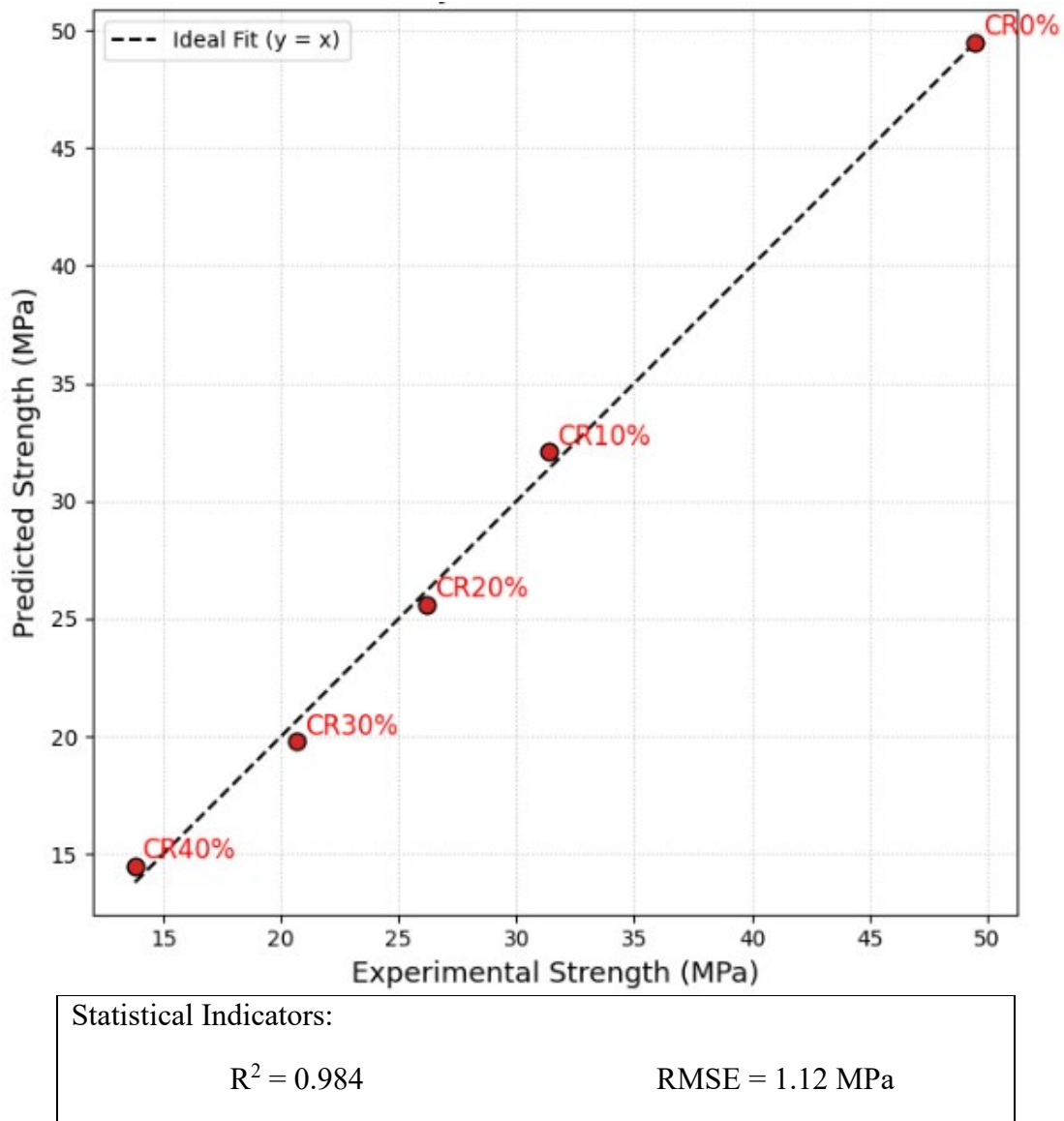


**Figure 10:** Experimental vs Predicted Compressive Strength (28-days, Normalized to CR0)

### 3.5.3 Split Tensile Strength Modeling (28 Days)

The formulation of a quadratic regression model to explain the relationship between the level of 28-day split tensile strength and the amount of CR added, as measured over five experimental data points, resulted in a  $R^2$  value of 0.972 and a root mean square error (RMSE) of 0.11 MPa. These statistical results indicate a high degree of agreement between the predicted and observed experimental results within the limits of experimental variability ( $\pm$ SD). The

absolute error of prediction remained less than 0.10 MPa at each CR level, providing an excellent model for describing the degradation trend of the resistance to tension. However, the coefficients generated by the regression do not represent any mechanism by which tensile strength is produced. As this data set was very small, the model is purely a statistical model, and is not to be used for predicting results beyond those obtained from this experiment. A comparative illustration of both experimental and predicted split tensile strength is illustrated in Figure 11.

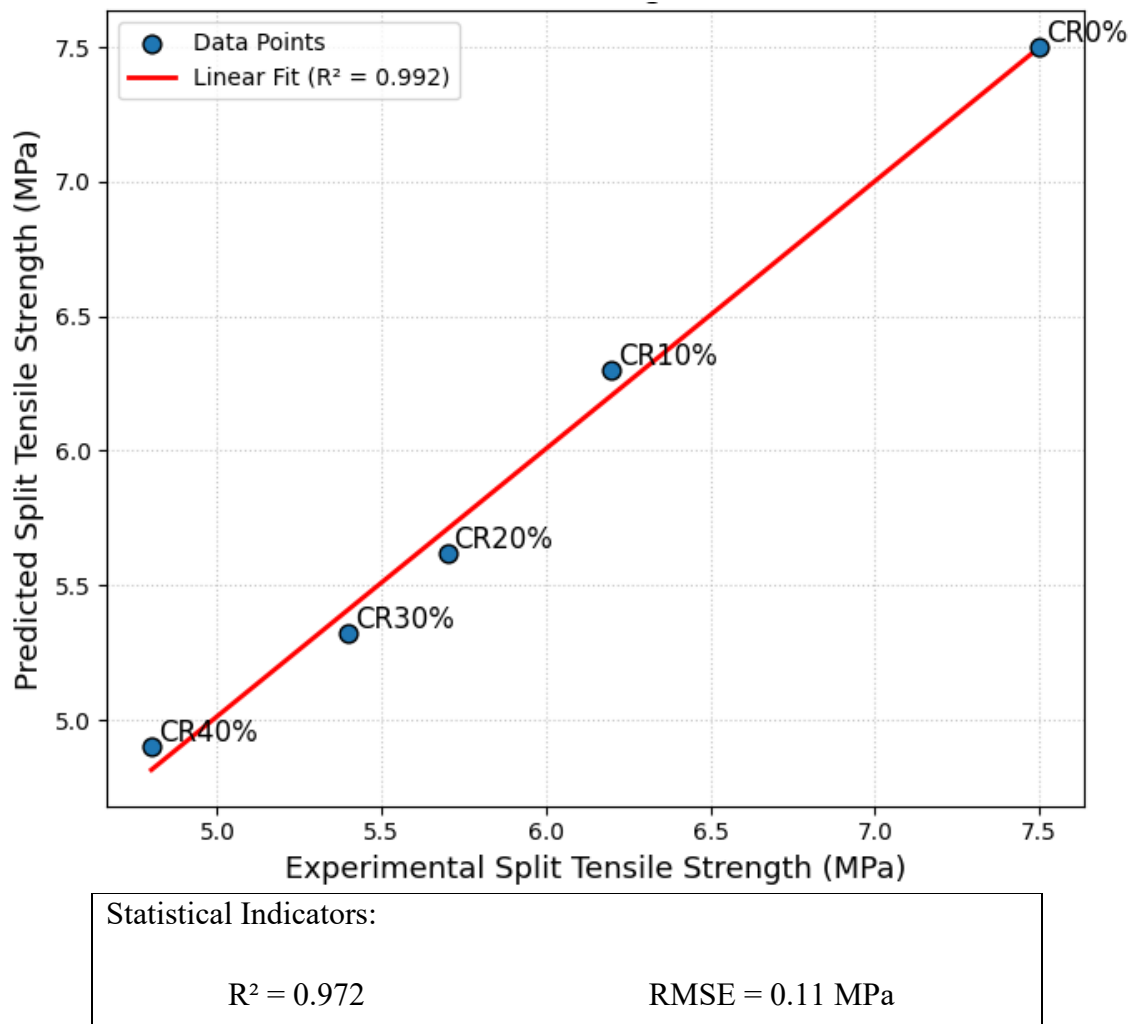


**Figure 11:** Experimental vs Predicted Split Tensile Strength

### 3.5.4 Flexural Strength Modeling (28 Days)

Quadratic regression modeling was used to predict the varying amounts of CR which influence the flexural strength at 28 days using 5 experimental data points. The model produced a good fit with  $R^2 = 0.965$ ,  $RMSE = 0.09$  MPa, therefore indicating a strong statistical relationship between the predicted and measured values of strength, within the SD of the data as shown in Figure 12. The maximum absolute error for any of the CR levels was  $\leq 0.10$  MPa indicating that there is a consistent trend in the data that supports the hypothesis. However, there is a reduction in flexural strength for varying amounts of CR. Because of the limited number of data points, one must be careful when interpreting the results of this regression analysis. The model provides a statistical estimate for flexural strength but does not identify mechanisms that

cause flexural strength; therefore, caution should be used in making predictions outside of the tested range.

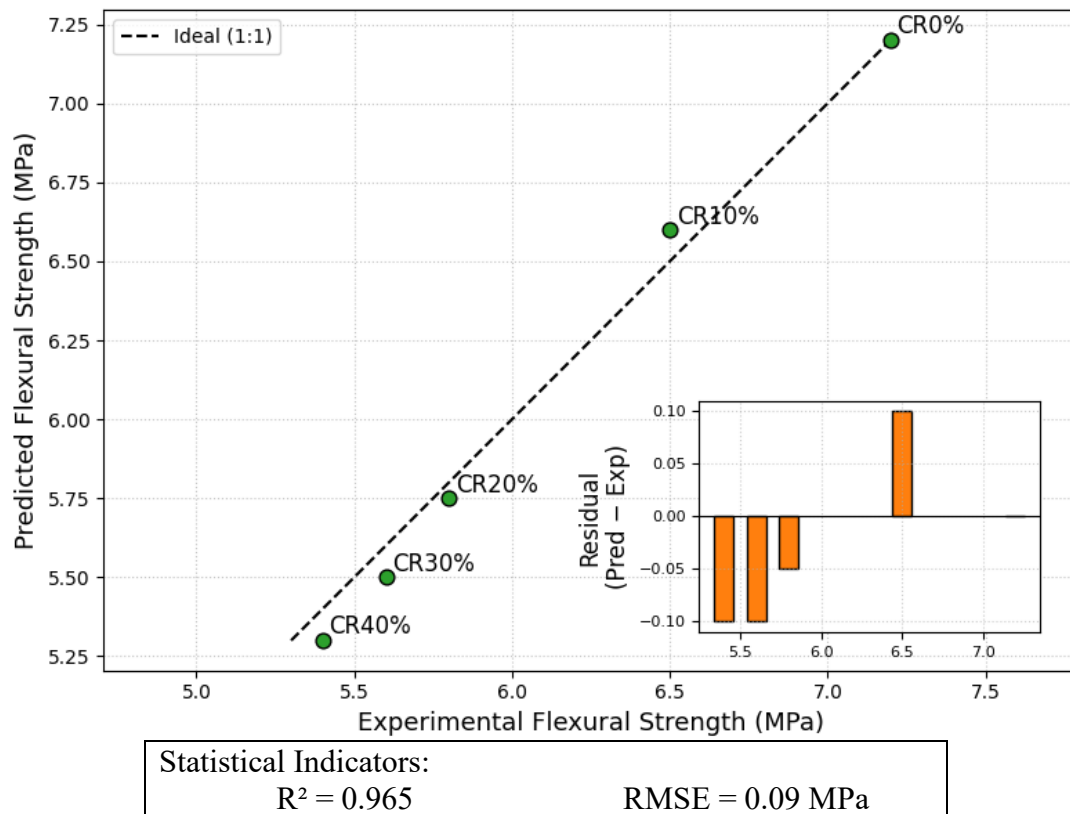


**Figure 12:** Experimental vs Predicted Flexural Strength Analysis with Residual Inset

### 3.6 Discussion

The combined examination of fresh and hardened properties indicates that the addition of CR to concrete maintains the deformability; however, the mechanical strength is gradually reduced, with the reduction greater than nominal values. The slump flow retention for all replacement levels was equal to or better than 100%, which confirms that all mixtures have the same capability to fill; however, the L-box ratios and stability indices indicate that the passing ability and cohesion were lower at the higher percentages of CR, particularly at 40% CR. Additionally, the performance of the hardened state has been shown to have a systematic decrease in strength, with the 28-day compressive strength retention reducing to 27.9% at 40% CR, while the tensile and flexural strength has exhibited less sensitivity. This indicates a direct trade-off between the ability to produce a workable mixture and the ability of a mixture to be structurally sound. From an application-based standpoint, the CR10 to CR20 mixtures represent a balanced compromise in that they exhibit adequate performance for all fresh properties and moderate retention of strength; however, there is no assertion of structural soundness for these mixes without further investigation into the durability, modulus, creep and bond properties associated with each mix. The nonlinear decrease in strength associated with increased amounts of CR has been quantitatively described by the models produced through predictive regression analysis; however, its five mix proportions limit its statistical generalization. Moreover, the lack of microstructural analysis precludes any mechanistic interpretation of the findings. Future efforts will benefit from the inclusion of microstructural examination of the mix designs and

an expansion of the dataset in order to develop strong relationships between structure and properties.

#### **4. CONCLUSIONS**

On the basis of the experimental results and statistical analysis, the following inferences can be made:

(1) The addition of CR to the concrete mix at a level of up to 40% of the total volume maintained a flowability and filling capability (as Defined by EFNARC's Slump Flow Standards). However, workability (passing ability and stability) decreased progressively with higher (>30%) CR levels, indicating that the mixtures have a significantly lower cohesive nature and an increased tendency for segregation.

(2) Compressive, split-tensile and flexural strength decreased with the increasing percentage of CR used as a partial replacement of the total volume of cement in the mix. The reduction in strength appears to be related to the lower rigidity of the CR particle and a weaker bond between the rubber and cement matrix rather than any tensile reinforcement or crack-bridging mechanism.

(3) The outcome shows that the controlled use of CR, especially at the 10-20% replacement rate, makes it possible to maintain an acceptable level of fresh-state properties and a significant amount of strength.

(4) This balanced reaction shows the technical feasibility of using a moderate amount of CR in mixtures where deformability, impact resistance, and sustainability are of prime importance compared to the compressive strength.

(5) The outcome shows the possibility of optimizing SCC mixtures for better workability and possible energy absorption properties.

(6) However, it is necessary to conduct a thorough durability test, elastic modulus, creep, and long-term performance evaluation before accepting it for structural use.

(7) Incorporating CR into concrete mixes provides an avenue for recycling waste tires and conserving materials used in the production of concrete. However, to achieve the sustainability benefits from using CR in concrete mixes, optimum levels of replacement must be attained, which will also accommodate the performance characteristics required of the final product.

(8) Additional data sets, as well as micro-structural studies, are required to establish structure–property relationships and correlations will provide useful predictive models.

#### **DECLARATIONS:**

##### **CONFLICT OF INTEREST**

They author declare that have no conflict of interest

##### **Ethical Approval**

Institutional Review Board approval was not required.

##### **Consent for Participate**

All contributors agreed and given consent to participate.

##### **Consent for Publication**

All contributors agreed and given consent to Publish.

##### **Data availability**

Data used in this research is confidential

## Competing interests

None

## Funding

The authors state that this work has not received any funding.

## Author Contribution

The authors confirm contribution to the paper as follows and all authors reviewed the results and approved the final version of the manuscript.

## Acknowledgements

The authors would like to thank the Deanship of Kalasalingam Academy of Research and Education for supporting this work.

## REFERENCE

- [1] Oyejobi, D., Firoozi, A., Fernández, D. B., & Avudaiappan, S. (2024). Integrating circular economy principles into concrete technology: Enhancing sustainability through industrial waste utilization. *Results in Engineering*, 24, 102846. <https://doi.org/10.1016/j.rineng.2024.102846>
- [2] Abera, Y. A. (2024). Sustainable building materials: A comprehensive study on eco-friendly alternatives for construction. *Composites and Advanced Materials*, 33. <https://doi.org/10.1177/26349833241255957>.
- [3] Suarez-Riera, D., Restuccia, L., Falliano, D., Ferro, G. A., Tuliani, J., Pavese, M., & Lavagna, L. (2024). An overview of methods to enhance the environmental performance of Cement-Based Materials. *Infrastructures*, 9(6), 94. <https://doi.org/10.3390/infrastructures9060094>.
- [4] Mayer, P. M., Moran, K. D., Miller, E. L., Brander, S. M., Harper, S., Garcia-Jaramillo, M., Carrasco-Navarro, V., Ho, K. T., Burgess, R. M., Hampton, L. M. T., Granek, E. F., McCauley, M., McIntyre, J. K., Kolodziej, E. P., Hu, X., Williams, A. J., Beckingham, B. A., Jackson, M. E., Sanders-Smith, R. D., . . . Mendez, M. (2024). Where the rubber meets the road: Emerging environmental impacts of tire wear particles and their chemical cocktails. *The Science of the Total Environment*, 927, 171153. <https://doi.org/10.1016/j.scitotenv.2024.171153>.
- [5] Kumar, A., Dhanorkar, R. J., Mohanty, S., & Gupta, V. K. (2024). Advances in recycling of waste vulcanized rubber products via different sustainable approaches. *Materials Advances*, 5(19), 7584–7600. <https://doi.org/10.1039/d4ma00379a>
- [6] Kevin, B., Sarker, P. K., & Madhavan, M. K. (2025). Performance assessment and microstructural characterization of combined surface, chemical and polymer treated crumb rubber concrete. *Scientific Reports*, 15(1), 15853. <https://doi.org/10.1038/s41598-025-97189-8>
- [7] Qureshi, M., Li, J., Wu, C., & Sheng, D. (2024). Mechanical strength of rubberized concrete: Effects of rubber particle size, content, and waste fibre reinforcement. *Construction and Building Materials*, 444, 137868. <https://doi.org/10.1016/j.conbuildmat.2024.137868>
- [8] Pham, T. M., Renaud, N., Pang, V., Shi, F., Hao, H., & Chen, W. (2021). Effect of rubber aggregate size on static and dynamic compressive properties of rubberized concrete. *Structural Concrete*, 23(4), 2510–2522. <https://doi.org/10.1002/suco.202100281>.
- [9] Saad, A. G., Sakr, M. A., Khalifa, T. M., & Darwish, E. A. (2024). Structural Performance of Concrete Reinforced with Crumb Rubber: A Review of Current

- Research. Iranian Journal of Science and Technology Transactions of Civil Engineering, 49(4), 3211–3254. <https://doi.org/10.1007/s40996-024-01629-w>
- [10] Kanagaraj, B., Ss, R., Ashutosh, Anand, N., & Lubloy, E. (2025). Engineering and sustainability characteristics of concrete blended with waste rubber crumbs as an alternate to conventional coarse aggregate. *Cleaner Waste Systems*, 11, 100271. <https://doi.org/10.1016/j.clwas.2025.100271>
- [11] Saif, Y., Mallek, J., Hadrich, B., & Daoud, A. (2025). Mechanical behavior of Self-Compacting concrete incorporating rubber and recycled aggregates for Non-Structural applications: Optimization using response surface methodology. *Buildings*, 15(15), 2736. <https://doi.org/10.3390/buildings15152736>
- [12] Qadir, I. M. A., & Noaman, A. T. (2024). Effect of combination between hybrid fibers and rubber aggregate on rheological and mechanical properties of self-compacting concrete. *Construction and Building Materials*, 414, 135038. <https://doi.org/10.1016/j.conbuildmat.2024.135038>
- [13] Tiza, M. T., Imoni, S., Akande, E. O., Mogbo, O., Jiya, V. H., & Onuzulike, C. (2024). Revolutionizing Infrastructure Development: Exploring Cutting-Edge advances in civil engineering materials. *Recent Progress in Materials*, 06(03), 1–68. <https://doi.org/10.21926/rpm.2403023>
- [14] Prithiviraj, C., Saravanan, J., Kumar, D. R., Murali, G., Vatin, N. I., & Swaminathan, P. (2022). Assessment of strength and durability properties of Self-Compacting concrete comprising alccofine. *Sustainability*, 14(10), 5895. <https://doi.org/10.3390/su14105895>
- [15] Boutlikht, M., Douadi, A., Khitas, N. E. H., Messai, A., Hebbache, K., Belebchouche, C., Smarzewski, P., & Tawfik, T. A. (2025). Optimizing of Self-Compacting Concrete (SCC): Synergistic impact of marble and limestone Powders—A Technical and Statistical analysis. *Buildings*, 15(7), 1043. <https://doi.org/10.3390/buildings15071043>
- [16] Sobuz, M. H. R., Aditto, F. S., Datta, S. D., Kabbo, M. K. I., Jabin, J. A., Hasan, N. M. S., Khan, M. M. H., Rahman, S. M. A., Raazi, M., & Zaman, A. a. U. (2024). High-Strength Self-Compacting concrete production incorporating supplementary cementitious materials: experimental evaluations and machine learning modelling. *International Journal of Concrete Structures and Materials*, 18(1). <https://doi.org/10.1186/s40069-024-00707-7>
- [17] Kelechi, S. E., Adamu, M., Mohammed, A., Ibrahim, Y. E., & Obianyo, I. I. (2022). Durability Performance of Self-Compacting concrete containing crumb rubber, fly ash and calcium carbide waste. *Materials*, 15(2), 488. <https://doi.org/10.3390/ma15020488>
- [18] Singh, G., Tiwary, A. K., Singh, S., Kumar, R., Chohan, J. S., Sharma, S., Li, C., Sharma, P., & Deifalla, A. F. (2022). Incorporation of silica fumes and waste glass powder on concrete properties containing crumb rubber as a partial replacement of fine aggregates. *Sustainability*, 14(21), 14453. <https://doi.org/10.3390/su142114453>
- [19] Hamzehkolaei, N. S., & Afshoon, I. (2025). Experimental investigation of mechanical properties and durability of SFR-SCC incorporating ceramic waste powder and coarse aggregates. *Multiscale and Multidisciplinary Modeling Experiments and Design*, 8(5). <https://doi.org/10.1007/s41939-025-00855-7>
- [20] Rahim, N. I., Mohammed, B. S., Abdulkadir, I., & Dahim, M. (2022). Effect of crumb rubber, fly ash, and nanosilica on the properties of Self-Compacting Concrete using response surface Methodology. *Materials*, 15(4), 1501. <https://doi.org/10.3390/ma15041501>
- [21] Uche, O. A., Kelechi, S. E., Adamu, M., Ibrahim, Y. E., Alanazi, H., & Okokpujie, I. P. (2022). Modelling and optimizing the durability performance of self consolidating concrete incorporating crumb rubber and calcium carbide residue using response surface methodology. *Buildings*, 12(4), 398. <https://doi.org/10.3390/buildings12040398>

- [22] EFNARC. (2005). *Specification and Guidelines for Self-Compacting Concrete*. European Federation of National Associations Representing for Concrete, Surrey, UK
- [23] ASTM International. (2019). *ASTM C78/C78M – Standard Test Method for Flexural Strength of Concrete (Using Simple Beam with Third-Point Loading)*. West Conshohocken, PA, USA.